Mutual Inhibition of RecQ Molecules in DNA Unwinding*

Bing-Yi Pan[‡]**, Shuo-Xing Dou**[‡1]**, Ye Yang**[‡]**, Ya-Nan Xu**[‡§]**, Elisabeth Bugnard**[¶‖]**, Xiu-Yan Ding**[‡]**, Lingyun Zhang**[‡]**, Peng-Ye Wang**[‡]**, Ming Li**[‡]**, and Xu Guang Xi**[¶2]

From the [‡]Key Laboratory of Soft Matter Physics and Beijing National Laboratory for Condensed Matter Physics, Institute of Physics, Chinese Academy of Sciences, Beijing 100190, China, the [§]Department of Physics, Renmin University, Beijing 100872, China, [¶]CNRS, UMR 3348, Institut Curie, Section de Recherche, Centre Universitaire, Bâtiment 110, F-91405 Orsay, France, and the [‖]Faculté de Pharmacie, Université Paris-sud 11, 5 rue JB Clément, 92296 Chatenay-Malabry Cedex, France

Helicases make conformational changes and mechanical movements through hydrolysis of NTP to unwind duplex DNA (or RNA). Most helicases require a single-stranded overhang for loading onto the duplex DNA substrates. Some helicases have been observed to exhibit an enhanced unwinding efficiency with increasing length of the single-stranded DNA tail both by preventing reannealing of the unwound DNA and by compensating for premature dissociation of the leading monomers. Here we report a previously unknown mutual inhibition of neighboring monomers in DNA unwinding by the monomeric *Escherichia coli* RecQ helicase. With single molecule fluorescence resonance energy transfer microscopy, we observed that the unwinding initiation of RecQ at saturating concentrations was more delayed for a long rather than a short tailed DNA. In stopped-flow kinetic studies under both single and multiple turnover conditions, the unwinding efficiency decreased with increasing enzyme concentration for long tailed substrates. In addition, preincubation of RecQ and DNA in the presence of 5′-adenylyl-β,γ-imidodiphosphate was observed to alleviate the inhibition. We propose that the mutual inhibition effect results from a forced closure of cleft between the two RecA-like domains of a leading monomer by a trailing one, hence the forward movements of both monomers are stalled by prohibition of ATP binding to the leading one. This effect represents direct evidence for the relative movements of the two RecA-like domains of RecQ in DNA unwinding. It may occur for all superfamily I and II helicases possessing two RecA-like domains.

Helicases hydrolyze NTP to translocate along ssDNA[3] and unwind dsDNA (or RNA) (1–5). The helicase activity relies on a chemical to physical energy transfer process that is achieved via conformational changes guided by nucleotide state transitions. Available crystal structures have revealed that superfamily I and II helicases contain two RecA-like domains and the NTP binding site is located in a cleft between the two domains (5, 6). Almost all signature motifs of the two superfamily helicases are clustered at the NTP binding site and around the bound DNA (5), implying a closely related mechanochemical coupling pathway in these helicases. Furthermore, the cleft between the two domains and the mode of their interaction with DNA vary with the nucleotide state (7, 8), supporting that the helicases translocate along ssDNA in an inchworm manner: the two domains move relative to each other while alternatively having tight and loose interactions with DNA. The step size of 1 nt estimated according to kinetic studies is consistent with such a mechanism (9, 10).

In general, helicases require a single-stranded overhang for loading onto the dsDNA substrate before they unwind the dsDNA. Various kinetic studies have shown that many helicases, such as NS3h (11), UvrD (12, 13), Dda (14), RecQ (15), and PcrA (16), unwind DNA more efficiently with increasing length of the ssDNA. The reasons are obvious: the additionally bound molecules may prevent the reannealing of the partially unwound DNA. In addition, for a helicase with limited processivity, the additional molecules may continue the unwinding if the functioning unit at the ss/dsDNA junction dissociates prematurely from the DNA substrate. But it is not very clear whether other types of interaction exist between the helicase active units (monomers, dimers, or hexamers) in DNA unwinding.

Escherichia coli RecQ is the first member of an important helicase family named after it. RecQ family helicases belong to superfamily II and play important roles in maintaining genomic stability (17, 18). Defects in three of the five RecQ family members in humans, WRN, BLM, and RECQ4, lead to human genetic diseases, Werner, Bloom, and Rothmund-Thomson syndromes, respectively (17, 18). Increasing evidence suggest that RecQ helicases act at multiple steps in DNA metabolisms, including stabilization of replication forks and removal of DNA recombination intermediates, to maintain genome integrity. As a prototype of the family, *E. coli* RecQ has been widely studied previously. DNA unwinding kinetic analyses demonstrate that *E. coli* RecQ may be active as monomers (15, 19). Crystal structures of its helicase core show that the two RecA-like domains are similar to that of superfamily I helicases such as Rep and PcrA (20). Thus it is very probable that RecQ translocates along ssDNA and unwinds dsDNA in an inchworm manner.

In this work we present our observation of a mutual inhibition effect of neighboring monomers in DNA unwinding of

[3] The abbreviations used are: ssDNA, single-stranded DNA; dsDNA, double-stranded DNA; nt, nucleotide(s); PEG, polyethylene glycol; FRET, fluorescence resonance energy transfer; AMPPNP, 5′-adenylyl-β,γ-imidodiphosphate; CCD, charge-coupled device.

E. coli RecQ. In both single molecule and stopped-flow kinetic experiments, the helicase activity was reduced rather than enhanced for a duplex DNA with a long 3′-ssDNA tail compared with that with a short tail. The additionally bound RecQ monomers inhibited the active helicase monomer at the ss/dsDNA junction. This effect very probably arises from an impediment of ATP binding to the leading active monomer by the trailing one. It is direct evidence for the relative movements of the two RecA-like domains of RecQ in DNA unwinding. In principle, the inhibition effect may be ubiquitous to both superfamily I and II helicases.

MATERIALS AND METHODS

Reagents and Buffers—All chemicals were reagent grade, and all buffers were prepared in ultrapure water from a Milli-Q water purification system (Millipore) having resistivity greater than 18.2 $M\Omega \cdot cm$. As in our previous stopped-flow kinetic studies (15), all the present unwinding reactions were performed at 25 °C and in buffers containing 25 mM Tris-HCl (pH 7.5 at 25 °C), 50 mM NaCl, 1 mM $MgCl_2$, and 0.1 mM dithiothreitol. The only difference is that the ATP concentrations used in the present study were varied rather than remaining constant (1 mM).

RecQ Protein and Oligonucleotide Substrates—*E. coli* RecQ protein was expressed and purified as described (19). Its purity was determined by SDS-PAGE analysis and found to be >95%. The DNA substrates used in the single molecule unwinding studies were 5′-ATC CGT CGA GCA GAG TCy5(dT$_N$)-3′ and 5′-Cy3-ACT CTG CTC GAC GGA T-3′ Biotin. Cy3 and Cy5 were incorporated in phosphoramidite forms, and biotin was added as BiotinTEG CPG during oligonucleotide synthesis. DNA substrates used in the bulk unwinding assays had both strands labeled with fluorescein (F) and hexachlorofluorescein (H), respectively. Their structures and sequences are 5′-CTC TGC TCG ACG GAT T-F-3′ and 5′-H-AAT CCG TCG AGC AGA G(dT$_N$)-3′, respectively. The protein trap used in the single turnover kinetic experiments was a 56-nt poly(dT) (dT$_{56}$).

Single-stranded oligonucleotides, with or without labels, were purchased from the Shanghai Sangon Biological Engineering Technology & Services Co., Ltd. (Shanghai, China), and all synthetic oligonucleotides were purified by high performance liquid chromatography. A 50 μM working stock of dsDNA was prepared by mixing equal concentrations of complementary single-stranded oligonucleotides in a 20 mM Tris-HCl buffer (pH 8.0 at 25 °C) containing 100 mM NaCl, followed by heating to 90 °C. After equilibrating for 3 min, annealing was allowed by slow cooling to room temperature.

Surface and Sample Cell Preparations for Single Molecule Assays—PEG surfaces that contain a small fraction (~1%) of biotinylated PEG molecules were prepared using almost the same procedure as described previously (21, 22). In brief, first, the glass coverslips and quartz slides were soaked in a 1% (v/v) solution of an amino-silane reagent (Vectabond, Vector Labs) in acetone and then soaked for 3 h with a PEG solution, containing 10% (w/w) M-PEG-SPA M_r 5000 (Nektar Therapeutics) and 0.1% (w/w) biotin-PEG-SPA M_r 3400 (Nektar Therapeutics) in 0.1 M sodium bicarbonate (pH 8.3). After the surfaces were coated, a sample cell was constructed by putting the PEG-coated side of the coverslip over the PEG-coated side of the quartz slide separated by a 100-mm thick spacer (3M double sided tape). Two 0.9-mm diameter holes were drilled into the quartz slide to form the inlet and outlet. Remaining boundaries between the sample cell and outside were sealed using epoxy. Once constructed, the sample cells were kept in a dry environment.

Single Molecule Measurements—A wide-field total internal reflection fluorescence microscope based on an inverted microscope (IX-71, Olympus) was used to image an area of 50×100 μm to an intensified digital CCD camera (I-PentaMAX-512EFT, Roper Scientific). Molecules were excited using a Nd:YVO$_4$ laser at 532 nm (Verdi-2, Coherent) through a quartz prism placed over a quartz slide via a thin layer of immersion oil. The incident angle of the laser was controlled to achieve total internal reflection at the interface between the quartz slide and aqueous imaging buffer. Fluorescently labeled DNA molecules are attached to this interface. Fluorescence signal was collected using a water immersion objective (Olympus UplanSApo $\times$60, 1.2 numerical aperture).

After rejecting the scattered laser light using a holographic notch filter at 532 nm (HNPF-532.0, Kaiser Optical Systems, Inc.), the imaging area was defined using a vertical slit located at the imaging plane of the microscope. The emission was subsequently collimated using a 20-cm focal length achromat lens (China Daheng Group, Inc.), split by a long pass extended reflection dichroic mirror at 610 nm (610DCLP, Chroma), recombined using an identical dichroic mirror after reflecting off a mirror each, and was finally imaged onto the intensified CCD using another 20-cm focal length achromat lens. To further reduce the cross-talk of signals, two band-pass filters were used in the two signal channels for Cy3 (S568/50M, Chroma) and Cy5 (D675/50M, Chroma). Donor Cy3 and acceptor Cy5 images were laterally displaced and each occupied one-half of the intensified CCD. Each fluorescent spot in the donor channel has a corresponding one in the acceptor channel, coming from the same DNA in the sample. All images were acquired with MetaMorph software (Universal Imaging).

In the experiments, the sample cell was first fixed on the stage of the microscope. Then streptavidin (Roche Applied Science) was added followed by the addition of 30–50 pM biotinylated Cy3- and Cy5-labeled DNA substrate. After washing off the unbound DNA, immobilized DNA was imaged in the unwinding buffer. To reduce the photobleaching effect, an oxygen scavenger system (0.1 mg/ml of glucose oxidase, 0.02 mg/ml of catalase, 1% β-mercaptoethanol, and 0.4% (w/w) β-D-glucose) was used to increase photostability of the fluorophores. Unwinding reaction was initiated by the simultaneous addition of RecQ and ATP.

Stopped-flow Kinetic Measurements—All the stopped-flow kinetic DNA unwinding assays were carried out using a Biologic SFM-400 mixer and a MOS450/AF-CD optical system, as described previously (15). The unwinding processes were observed by monitoring the fluorescence signal change of fluorescein at 525 nm due to the disruption of FRET between fluorescein and hexachlorofluorescein as the two molecules are separated. The unwinding efficiencies were obtained by calibration measurements as described (15).
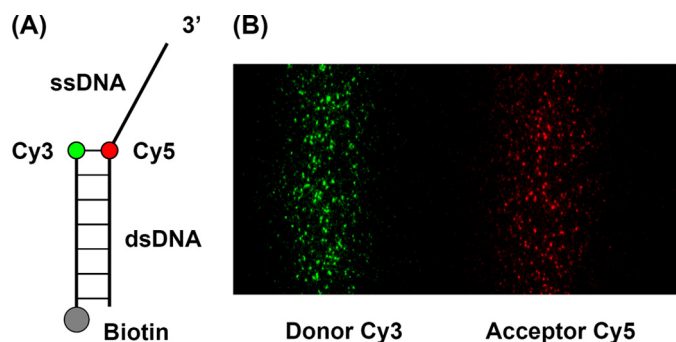
FIGURE 1. **Single molecule fluorescence assay for DNA unwinding.** *A*, schematic illustration of the structure of the 16-bp DNA substrate used in our experiments. The donor (Cy3) and acceptor (Cy5) fluorescent molecules are located at the ss/dsDNA junction. The DNA substrate is tethered to the PEG-coated quartz surface with biotin. *B*, a typical CCD image (pseudo-colored) of the Cy3 and Cy5 channels. Cy3- and Cy5-labeled DNA molecules immobilized to the quartz surface give rise to hundreds of fluorescent spots in both imaging channels.

In the bulk DNA unwinding assays, the ATP concentration might be significantly reduced or even depleted due to continuous hydrolysis by the helicase, especially when the ATP concentration was low. To avoid any effect in this aspect, 20 mM phosphocreatine and creatine phosphokinase (30 units/ml) were added in the reaction buffers in all bulk measurements.

For the dissociation kinetic assay of the helicase from DNA substrate, the helicase was preincubated with the DNA substrate (labeled only with fluorescein) in one syringe, whereas the protein trap (dT_{56}) together with or without the nucleotide cofactor AMPPNP were preincubated in another syringe. The reaction was initiated by rapid mixing of the two syringes. The sample was excited at 492 nm and anisotropy was monitored at 525 nm. Decreasing of the fluorescence anisotropy reflected the helicase dissociation process.

RESULTS AND DISCUSSION

Unwinding Initiation Is Retarded for Long Tailed DNA Substrate—We used a single molecule FRET assay, similar to that used by Ha *et al.* (21), to observe the unwinding of individual DNA molecules. The DNA substrate was a 16-bp duplex DNA with a 3′-ssDNA tail. The donor (Cy3) and acceptor (Cy5) fluorophores were attached at the ss/dsDNA junction (Fig. 1*A*). The DNA was tethered to a polymer-passive quartz surface via biotin. The Cy3 and Cy5 fluorescence signals were separated but simultaneously detected with an intensified CCD (Fig. 1*B*).

After addition of a RecQ and ATP solution (20 μl), a characteristic time (defined as initiation time) elapsed before we observed opposite changes of the Cy3 and Cy5 signals and a corresponding FRET decrease that was caused by the increase in interfluorophore distance as the DNA was unwound (Fig. 2). Here the time it took for FRET efficiency to drop from the high to low levels was defined as *partial* unwinding time because, as will be seen later, this FRET efficiency change may not correspond to a complete unwinding of the whole DNA duplex.

At a fixed ATP concentration, we observed that the initiation time for the 20-nt 3′-ssDNA-tailed DNA substrate was longer than that for the 6-nt substrate (Fig. 3). At first glance, this seems to be reasonable as two or more RecQ monomers might bind to the long tail of the 20-nt substrate. If the monomer
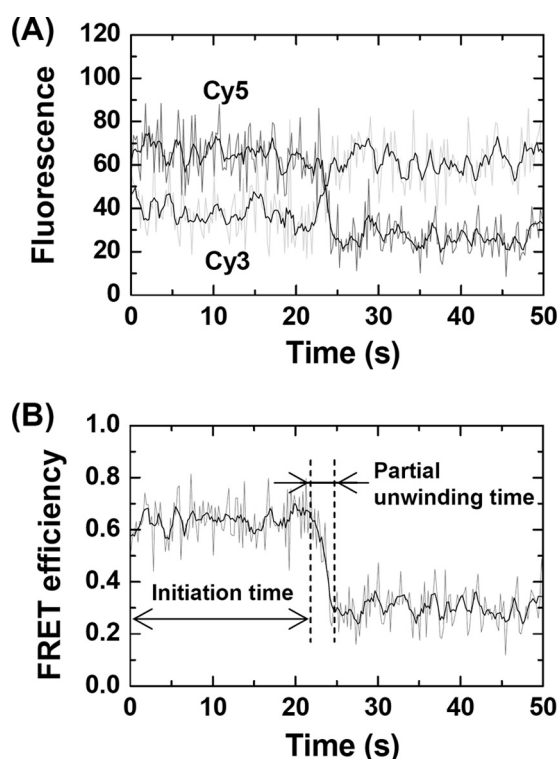

FIGURE 2. **Typical single molecule DNA unwinding time records for the 20-nt tailed 16-bp substrate.** The RecQ concentration used was 40 nM and ATP was 5 μM. *A*, fluorescence intensities of Cy3 and Cy5 (200 ms integration time). *B*, corresponding variation of the FRET efficiency. Definitions of the initiation and partial unwinding times are schematically shown. In both panels, the raw time traces are shown in *gray* and the 5-point averaged traces are in *black*.

pre-bound at the ss/dsDNA junction failed to initiate unwinding due to premature detachment, the other monomer(s) pre-bound farther away from the junction would translocate along the ssDNA to the junction and take on the unwinding task, thus resulting in a longer initiation time. We noticed, however, that the partial unwinding time (Fig. 4), although dependent on ATP concentration, was much shorter than the initiation time at a given ATP concentration. Assuming that the ssDNA translocation rate of RecQ is the same as the dsDNA unwinding rate (usually the former is much higher than the latter as can be known from available data for other helicases such as UvrD (23)), then the time it takes for the second (*i.e.* trailing) monomer to reach the ss/dsDNA junction by translocating along the ssDNA tail would be at most only several seconds, far from enough to account for the much prolonged unwinding initiation time.

We now think of another possible interpretation. Like other superfamily I and II helicases, RecQ has two RecA-like domains with the ATP binding site located between them (Fig. 5*A*) (20). According to crystal structures of PcrA and UvrD in complex with DNA (7, 8), the cleft between the two RecA-like domains is opened in the apo state and closed upon ATP binding. So what will happen if two RecQ monomers simultaneously bind to the ssDNA tail of the DNA substrate? The cleft in the leading helicase without bound ATP, originally in the open form, may be forced to close by the binding or forward movement of the trailing monomer (Fig. 5*B*). Then ATP access to the cleft of the
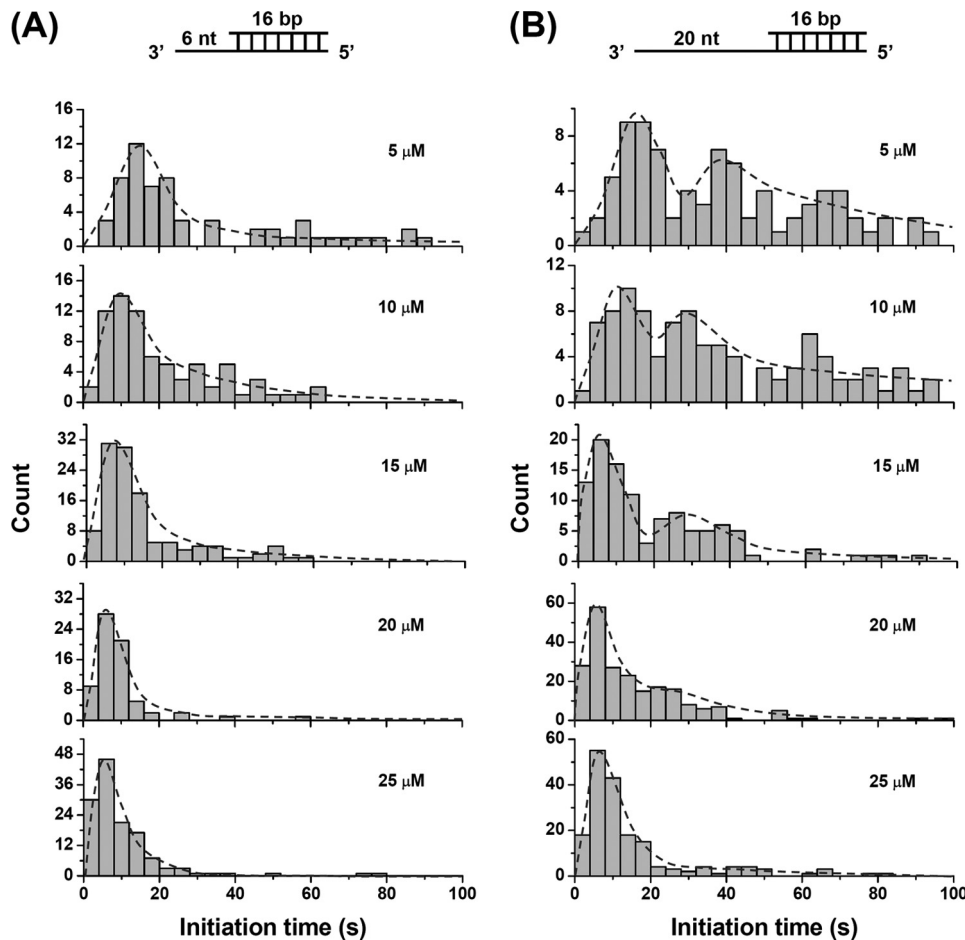
FIGURE 3. **Histograms of unwinding initiation time at different ATP concentrations.** The RecQ concentration used was 40 nM. *A,* 6-nt-tailed 16-bp substrate; *B,* 20-nt-tailed 16-bp substrate. The *dashed curves* are guidelines for the eyes.
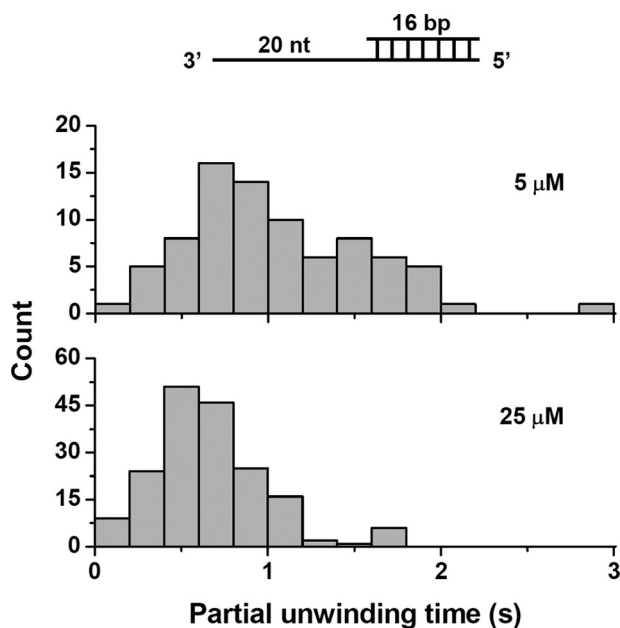

FIGURE 4. **Histograms of partial unwinding time at two different ATP concentrations for the 20-nt-tailed 16-bp DNA substrate.** The RecQ concentration was 40 nM.

leading helicase would be significantly obstructed, resulting in a stall of forward movement for both helicases. The stall, however, may be temporary because the thermal fluctuations of the two RecA-like domains may provide the opportunity for ATP to bind. As easily imaginable, the lower the ATP concentration, the more difficult it is for the leading monomer to bind an ATP and restore the unwinding. As will be seen in the following bulk single turnover kinetic experiments, the mutual inhibition effect is indeed more obvious at low ATP concentrations.

Retardation Is Absent at a Low Enzyme Concentration—To verify the mutual inhibition effect hypothesis, we repeated the experiments at a lower RecQ concentration (10 nM). Our logic is that the probability should be much reduced for simultaneous binding of multiple RecQ monomers to the 20-nt ssDNA tail and thus the inhibition effect may be eliminated. As can be seen in Fig. 6, the situation was indeed changed: the initiation time for the 20-nt 3′-ssDNA-tailed DNA substrate became shorter than that for the 6-nt substrate.

Several points may be noticed by comparing the results in Figs. 3 and 6 at the same ATP concentration (10 μM). (i) The unwinding initiation times were similar for the two different RecQ concentrations in the case of the 6-nt-tailed substrate where the mutual inhibition effect is always absent. (ii) The unwinding initiation time was longer at a saturated RecQ concentration due to the mutual inhibition effect in the case of 20-nt-tailed substrate. (iii) At the low RecQ concentration, the initiation times for the two different substrates were expected to be similar as the mutual inhibition effect was absent in both cases, but actually they were quite different. As a helicase usually has low binding affinity for DNA substrates with short tails (24), one plausible explanation is that RecQ monomers bound more slowly (or less readily) to the short tailed substrate.

Unwinding Time Is Significantly Extended for Long Duplex Substrate—In principle, if the mutual inhibition effect exists for the two bound monomers at the moment of unwinding initiation, it should also exist during the DNA unwinding process because a helicase monomer translocating along ssDNA can easily catch up with a functional monomer at the ss/dsDNA junction. The 16-bp DNA substrate that we used before may be too short, or not suitable for observing the inhibition phenomenon during DNA unwinding. We therefore repeated the experiment using a longer DNA substrate. This substrate was a
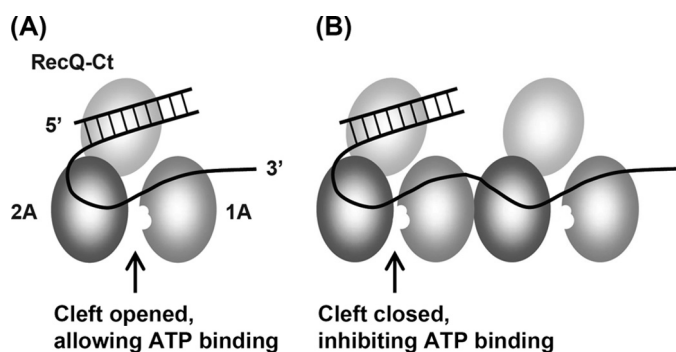
FIGURE 5. Proposed mechanism for the mutual inhibition effect of RecQ. *1A* and *2A* are the two RecA-like domains and *RecQ-Ct* is a domain conserved among RecQ family helicases. The ATP binding site is located in the cleft between the *1A* and *2A* domains as indicated. *A,* when the ssDNA tail of the substrate is short or the RecQ concentration is low, only one RecQ monomer is bound at the ss/dsDNA junction, in a manner as suggested previously. In the apo state, the cleft of the monomer is opened, allowing ATP binding to it. *B,* when the ssDNA tail of the substrate is long and the RecQ concentration is high enough, two RecQ monomers may be bound to the substrate, the leading one (*i.e.* the left one) at the ss/dsDNA junction and the trailing one (*i.e.* the right one) near the end of the ssDNA tail. The cleft in the leading monomer is made closed by either DNA binding (as schematically shown) or forward movement of the trailing one, thus ATP binding to it is inhibited.
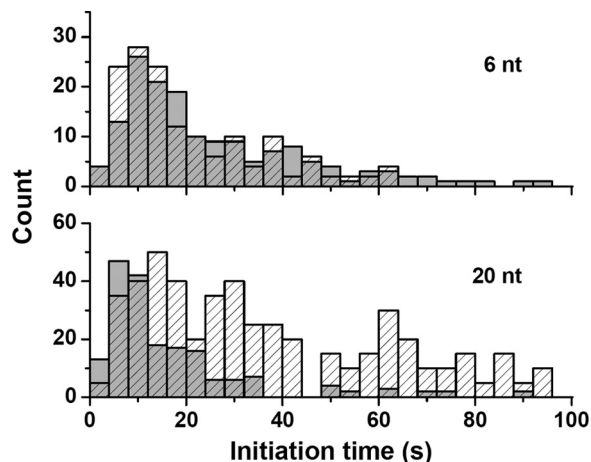

FIGURE 6. Histograms of unwinding initiation time for 6- and 20-nt-tailed 16-bp substrates. The ATP concentration was 10 μM and RecQ was 10 nM. For comparison, the corresponding results with 10 μM ATP and 40 nM RecQ as previously shown in Fig. 3 were also presented (rescaled) in the *slashed columns.*

30-bp dsDNA with a 20-nt 3′ tail. In addition, the labeling positions of Cy3 and Cy5 were exchanged (see *inset* of Fig. 7*A*) so that the fluorescence signal of Cy3 would disappear as soon as the duplex was totally unwound.

Shown in Fig. 7 is a typical unwinding time course observed in the experiment. In this case, the unwinding started at ~6 s. But then, the Cy3-labeled ssDNA remained there until ~55 s. This implies that a complete unwinding of the whole duplex took as long as ~49 s. So what happened? We may imagine that when the unwinding was started at ~6 s by a RecQ monomer, Cy3 fluorescence was quickly increased and Cy5 fluorescence was quickly decreased due to fast separation of the two fluorophores. But what happened now is that another monomer caught up with the functional monomer and caused a stall of the unwinding. As the two fluorophores were still separated by the two monomers, their fluorescence did not change. The stall would be terminated and the unwinding reinitiated as soon as
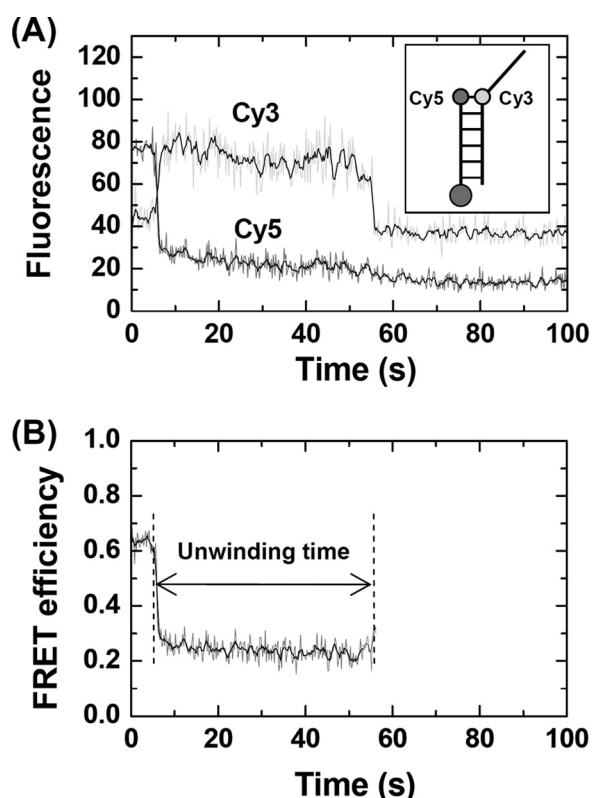

FIGURE 7. Typical single molecule DNA unwinding time records with a 20-nt-tailed 30-bp DNA substrate. The RecQ and ATP concentrations were 40 nM and 10 μM, respectively. *A,* fluorescence intensities of Cy3 and Cy5 (200 ms integration time). After the Cy3-labeled ssDNA diffused away at ~55 s, the measured fluorescence intensity was contributed by background noise. *Inset,* schematic illustration of the structure of the 30-bp DNA substrate. *B,* corresponding variation of FRET efficiency. Definition of the unwinding time is schematically shown. In both panels, the raw time traces are shown in *gray* and the 5-point averaged traces are in *black.*

ATP bound to the first monomer or one of the two monomers dissociated. Finally, the whole duplex was totally unwound and the Cy3-labeled ssDNA segment was diffused away at 55 s. It is not difficult to imagine that before unwinding the whole duplex was finished, events of partial unwinding and temporary stall might have alternatively occurred several times accompanied with the dynamic binding and dissociation of the helicase monomers.

According to the above analysis, the time interval between the fluorescence jump and drop of Cy3 was defined as the unwinding time in the present experiment. The distributions of unwinding time at different ATP concentrations are given in Fig. 8. Clearly, the present unwinding time was much longer than that expected for the 30-bp substrate based on the unwinding time for the 16-bp substrate (Fig. 4). In addition, the unwinding time decreased with increasing ATP concentration, consistent with the idea that the inhibition effect is less serious or the stall time shorter at higher ATP concentrations.

It is worth emphasizing that the fluorescence drop of Cy3 as shown in Fig. 7*A* could not be caused by re-annealing the two ssDNA generated by unwinding because the fluorescence of Cy5 did not show a corresponding rise. It was not caused by photobleaching either, because the time interval between the fluorescence jump and drop of Cy3 depended on ATP concen-
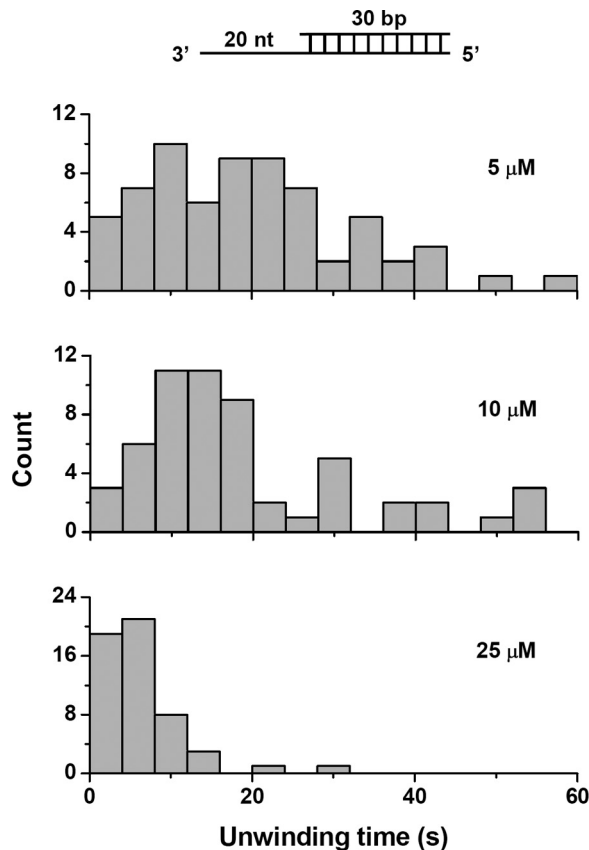
FIGURE 8. **Histograms of unwinding time at three different ATP concentrations for the 20-nt-tailed 30-bp DNA substrate.** The RecQ concentration was 40 nM.

FIGURE 9. **Multiple turnover DNA unwinding at different RecQ concentrations.** 2 nM DNA substrate was first preincubated with RecQ of the indicated concentrations in the reaction buffer at 25 °C for 5 min and the unwinding reaction was initiated by adding 10 μM ATP. The kinetic time courses were fit with a double exponential, giving the unwinding amplitudes of the fast and slow phases. *A*, 6-nt-tailed 16-bp substrate. *B*, 20-nt-tailed 16-bp substrate.

tration (Fig. 8). In addition, our control showed that photobleaching was negligible in our experiments.

From the present experimental results with the 30-bp DNA substrate, we know that the drop of FRET efficiency from the high to low levels (Fig. 7*A*) resulted from a quick separation of Cy3 and Cy5 after initiation of DNA unwinding. Although the separation was large enough to disrupt FRET between the two fluorophores, the dsDNA was not unwound completely. That is why we used the term "partial unwinding time" in previous experiments with the 16-bp substrates (Fig. 2). Now one may wonder how much DNA duplex was unwound to cause a separation that was large enough to disrupt the FRET between Cy3 and Cy5. According to a theoretical prediction for FRET efficiency (25), a separation of 5 nm should be enough for such a disruption. With an ssDNA length per base of 0.4 nm, a 5-nm separation requires at least an unwinding of $5/2/0.4 = \sim6$ bp duplex DNA. Thus the actual time for unwinding the whole 16-bp substrate might be 2–3 times longer than that given in Fig. 4. But even so, the unwinding time is still much shorter than the observed initiation time (Fig. 3).

Amplitude of Fast Unwinding Phase Decreases with Increasing Enzyme Concentration under Multiple Turnover Unwinding Conditions—To study systematically the mutual inhibition effect, we then resorted to bulk stopped-flow kinetic measurements while using the same 6- and 20-nt-tailed 16-bp DNA substrates. First we carried out a DNA unwinding assay under
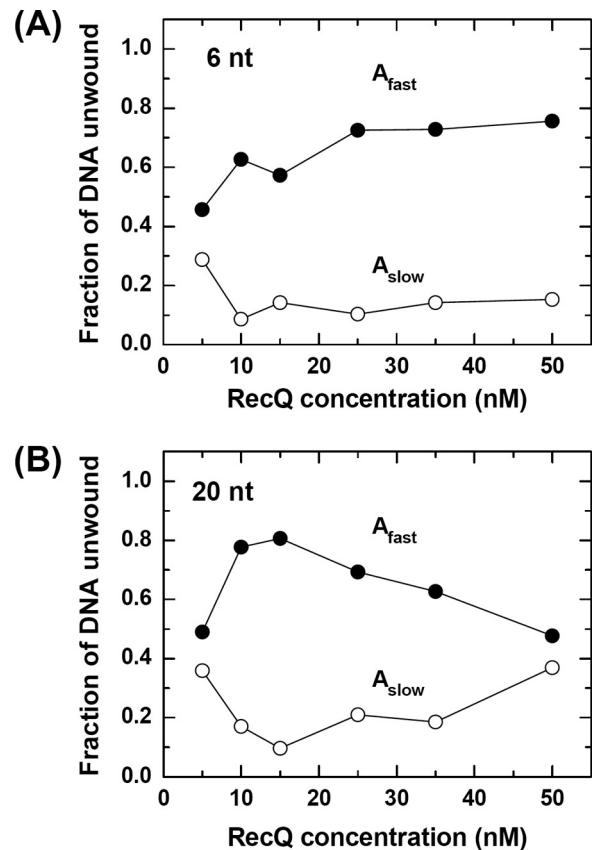
multiple turnover conditions similar to that in the above single molecule experiments.

In this assay, 2 nM DNA substrate was first preincubated with RecQ at a concentration varying from 5 to 60 nM in the reaction buffer at 25 °C for 5 min and the unwinding reaction was initiated by adding ATP. Under these conditions, we observed that the unwinding kinetics were biphasic for both 6- and 20-nt-tailed substrates (data not shown). From fitting of the unwinding curves, the amplitudes for the fast and slow phases as a function of RecQ concentration were obtained (Fig. 9).

For the 6-nt substrate, the amplitude for the fast phase A_{fast} increased with increasing RecQ concentration and then became saturated (at $\sim75\%$), whereas for the slow phase, A_{slow} showed a reversed trend: decreasing with increasing RecQ concentration and then was stabilized (at $\sim15\%$). For the 20-nt substrate the trends were somewhat different. A_{fast} first increased with increasing RecQ concentration, just like that for the 6-nt substrate. But after reaching a maximum ($\sim80\%$), A_{fast} started to decrease with a further increasing of RecQ concentration. As in the case of the 6-nt substrate, A_{slow} showed a reversed trend. These results are interesting. We think they may be understood as follows.

In the case of the 6-nt substrate, the DNA provided a single binding site for RecQ. As the fraction of DNA with a bound RecQ monomer before unwinding initiation (*i.e.* during the

preincubation process) would increase and then become saturated with increasing RecQ concentration, so did the fast phase that was contributed by the pre-bound monomers on the substrates. The slow phase was contributed by monomers that bound to the vacant substrates in the course of DNA unwinding. Thus it decreased with increasing RecQ concentration.

In the case of the 20-nt substrate, although the DNA tail provided several binding sites for RecQ, the situation should be similar as in the case of 6-nt substrate as long as the RecQ concentration was low enough such that on average only one or less than one RecQ monomer was bound to the ssDNA tail at any moment. But at higher RecQ concentrations, however, because emergence of the mutual inhibition effect, some pre-bound monomers could not move forward normally. It took longer time for these affected monomers to finish DNA unwinding, or even more seriously, these monomers might detach from the DNA substrate before arriving at the ss/dsDNA junction to start unwinding. Thus this part of pre-bound monomers could no longer contribute to the fast phase. Consequently, the fast phase of unwinding was reduced and the slow phase enhanced at high RecQ concentrations.

Note that here one may tend to think alternatively that the fast phase resulted simply from the RecQ monomers bound at the ss/dsDNA junctions and the slow phase from the other bound monomers. But if this is true, then the decrease of A_{fast} with increasing RecQ concentration could not be explained.

Unwinding Efficiency Is Reduced for Long Tailed DNA Substrate under Single Turnover Conditions—In the single Molecule experiments, it was observed that the mutual inhibition effect was more obvious at low ATP concentrations because the probability for ATP binding was more reduced. Here we performed a single turnover DNA unwinding kinetic assay to have a further investigation.

First a subsaturating enzyme concentration was used. 20 nM DNA substrate (6- or 20-nt tailed) was first preincubated with 7 nM RecQ in the reaction buffer at 25 °C for 5 min and the unwinding reaction was initiated by adding ATP of a varying concentration and 4 μM protein trap (dT$_{56}$). We observed that the unwinding amplitude with the 20-nt substrate was approximately equal or slightly higher than that with the 6-nt substrate at different ATP concentrations (Fig. 10A). As each DNA molecule was essentially bound at most with one RecQ monomer under these conditions, there would be no mutual inhibition effect, regardless of the tail length of substrate. Therefore, the slight difference should be simply due to a difference of binding affinity of the two substrates for RecQ, as was mentioned before.

Then we used a saturating enzyme concentration. 2 nM DNA substrate (6- or 20-nt tailed) was first preincubated with 35 nM RecQ in the reaction buffer at 25 °C for 5 min and the unwinding reaction was initiated by adding ATP and 2 μM protein trap (dT$_{56}$). Under these conditions, each 6-nt-tailed DNA molecule was still bound at most with one RecQ monomer, whereas each 20-nt-tailed DNA molecule could be bound with two or more RecQ monomers. At present, the unwinding amplitude for the 20-nt substrate was always lower than that for the 6-nt substrate, whereas the difference became less significant at high ATP concentrations (Fig. 10B). Note that if the mutual inhibi-
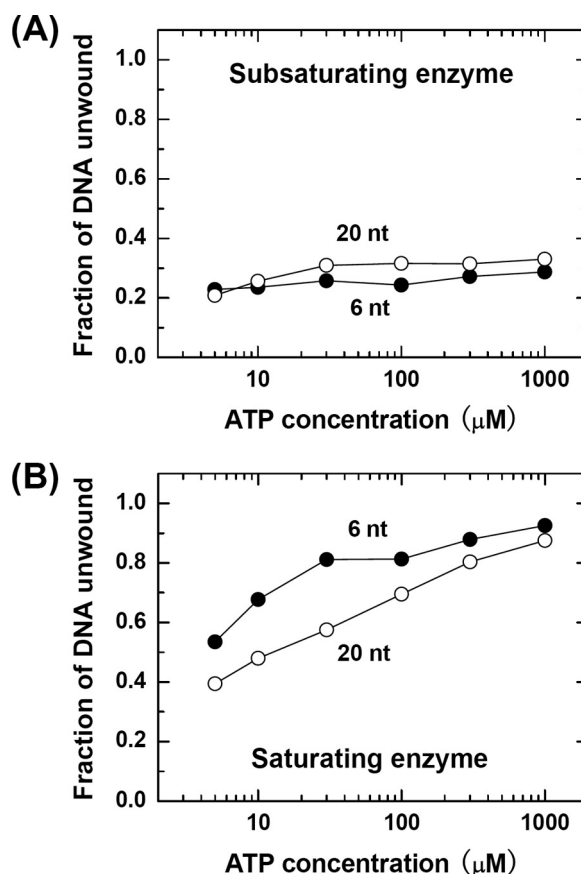

FIGURE 10. **Single turnover DNA unwinding at different ATP concentrations.** The DNA substrate (6- or 20-nt-tailed 16-bp duplex) was first preincubated with RecQ helicase in the reaction buffer at 25 °C for 5 min. The unwinding reaction was initiated by adding ATP and the excessive protein trap (dT$_{56}$), which prevents, after unwinding initiation, any free or dissociated RecQ molecules from rebinding to the duplex DNA substrates. *A*, unwinding amplitudes under subsaturating enzyme conditions (20 nM DNA, 7 nM RecQ, 4 μM dT$_{56}$). *B*, unwinding amplitudes under saturating enzyme conditions (2 nM DNA, 35 nM RecQ, 2 μM dT$_{56}$).

tion effect did not manifest, the amplitude for the 20-nt substrate could be much higher than that for the 6-nt substrate due to contribution of the additionally bound monomers as well as a higher affinity of the 20-nt substrate for RecQ binding.

Preincubation with AMPPNP Alleviates the Mutual Inhibition Effect—According to our proposal, the mutual inhibition effect results from a forced closure of the cleft between the two RecA-like domains of the leading RecQ monomer, prior to ATP binding, by the trailing monomer. Thus if the unnatural closure is prevented by some means, inhibition might be eliminated. One such means that we have conceived is to use the non-hydrolysable ATP analog AMPPNP. If AMPPNP is present during preincubation of DNA substrate and RecQ, it is expected that the cleft of the leading RecQ monomer with a bound AMPPNP molecule cannot be forced to close to the same extent as when in the apo state. Then after unwinding initiation by adding ATP, DNA unwinding may progress as soon as the leading monomer releases the pre-bound AMPPNP and then binds ATP. To verify the above assumption, we carried out single turnover unwinding kinetic experiments with AMPPNP.
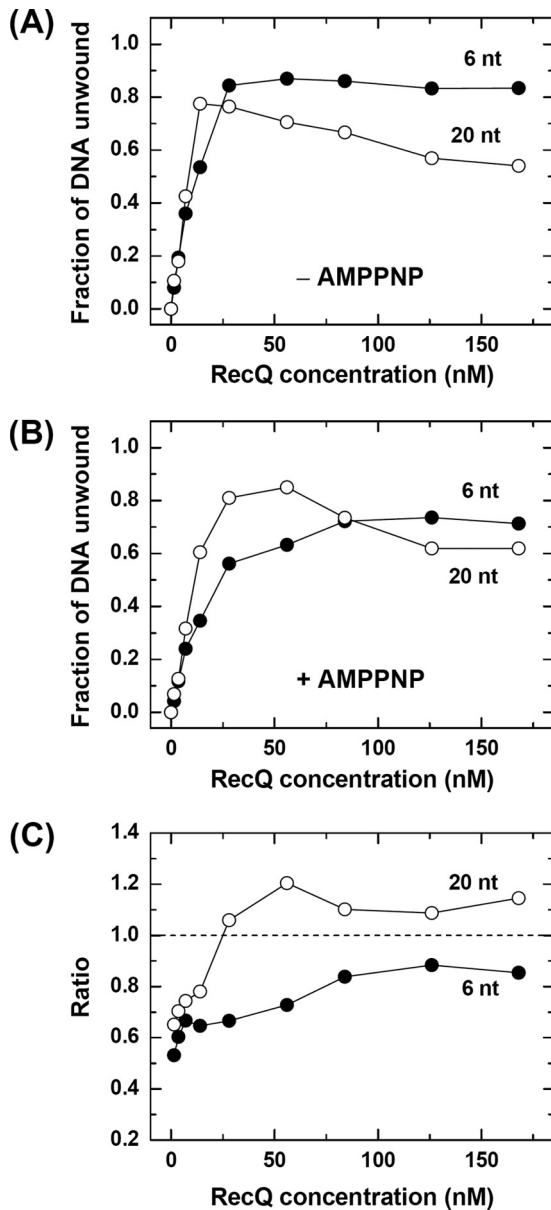
FIGURE 11. **Single turnover DNA unwinding in the absence or presence of AMPPNP.** 10 nm DNA substrate (6- or 20-nt-tailed 16-bp duplex) was first preincubated with RecQ helicase of varying concentrations in the reaction buffer with or without 1 μm AMPPNP at 25 °C for 5 min. The unwinding reaction was initiated by adding 30 μm ATP and 2 μm protein trap (dT$_{56}$). *A*, unwinding amplitudes in the absence of AMPPNP. *B*, unwinding amplitudes in the presence of AMPPNP. *C*, the ratio between the data in *A* and *B*.

As a control, we first carried our normal measurements without using AMPPNP. 10 nm DNA substrate (6- or 20-nt tailed) was first preincubated with RecQ at the indicated concentration in the reaction buffer at 25 °C for 5 min and the unwinding reaction was initiated by adding 30 μm ATP and 2 μm protein trap (dT$_{56}$). The unwinding amplitude as a function of RecQ concentration is given in Fig. 11*A*. For the 6-nt substrate, the unwinding amplitude first increased and then became saturated with increasing enzyme concentration. For the 20-nt substrate, the unwinding amplitude also increased first with increasing enzyme concentration. But after reaching a peak, it started to drop due to the mutual inhibition effect.

Then we repeated the experiments using AMPPNP. The experimental procedures were the same as above. The only difference was that 1 μm AMPPNP was added in the preincubation buffer for DNA and RecQ before unwinding initiation. As shown in Fig. 11*B*, the variation behavior of unwinding amplitude with the RecQ concentration was indeed changed by the presence of AMPPNP for both substrates. Especially, the range of RecQ concentration in which the unwinding efficiency for the 20-nt substrate was higher than that for the 6-nt substrate became much wider due to an alleviation of the mutual inhibition effect by AMPPNP.

To see more clearly, we plot the ratio of the data in Fig. 11*B* over that in Fig. 11*A* for each substrate (Fig. 11*C*). For the 6-nt substrate, the presence of AMPPNP could only reduce the unwinding efficiency. This may be easily understood because the helicase is needed, after addition of ATP, to release AMP-PNP first before binding ATP and starting the DNA unwinding. During the time for AMPPNP release, the helicase may dissociate from DNA. Note that, as the AMPPNP concentration was very low compared with ATP in the unwinding solution (1:30), the probability for RecQ to bind AMPPNP rather than ATP in the course of unwinding might be negligible.

For the 20-nt substrate, the presence of AMPPNP had the same effect of reducing the unwinding efficiency at low RecQ concentrations (<25 nm). It enhanced the unwinding efficiency, however, when the RecQ concentrations were higher and thus the mutual inhibition effect would appear. This demonstrates that AMPPNP indeed restrained effectively the inhibition effect as we imagined.

It should be mentioned that if the binding affinity of RecQ for the ss/dsDNA substrate is low in the AMPPNP state, then the unwinding efficiency of RecQ in the AMPPNP assay would be significantly compromised because of a much increased probability for dissociation of the AMPPNP-bound RecQ from DNA. From the actual results we may deduce that RecQ bound tightly to the substrate in the AMPPNP state. To see quantitatively the DNA binding characteristics of RecQ in apo and AMPPNP states, we used an fluorescence anisotropy method to measure directly the dissociation rates of RecQ from DNA.

We observed that dissociation from the 20-nt-tailed 16-bp ss/dsDNA substrate exhibited similar behaviors under conditions of the two different nucleotide states: occurring in two phases, a slow one and a fast one (Fig. 12). The slow phase described the actual dissociation process of the helicase from the ss/dsDNA junction. The fast phase should correspond to the dissociation process for helicase monomers that were bound less tightly to the end of the ssDNA tail. From the results, we know that RecQ bound to the ss/dsDNA junction three times more tightly in the AMPPNP (or ATP) state than in the apo state.

Inhibition Effect for Other Helicases with RecA-like Domains—The current available crystal structures of helicases indicate that all superfamily I and II helicases contain two RecA-like domains (5). Thus one may ask whether the mutual inhibition effect observed for RecQ exists for those other helicases. In light of the present results, we try to re-examine previous kinetic studies on DNA unwinding behaviors of different helicases.
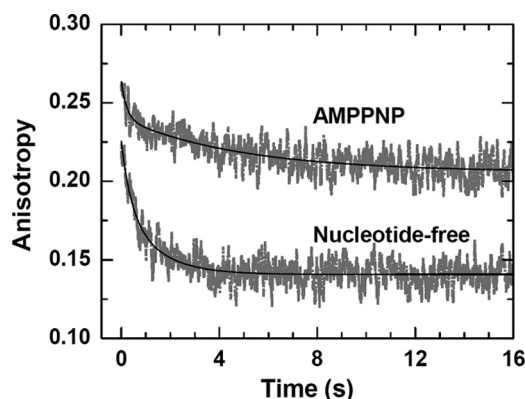
FIGURE 12. **Dissociation kinetics of bound RecQ helicase from DNA substrates in the absence or presence of AMPPNP.** 20 nM DNA substrate (20-nt-tailed 16-bp ss/dsDNA) was preincubated with 100 nM enzyme in the reaction buffer at 25 °C for 5 min and the reaction was initiated by adding 2 μM protein trap (dT_{56}) without or with 1 mM nucleotide cofactor AMPPNP. The data curve for AMPPNP was displaced vertically for clarity. The *solid lines* were double-exponential fits of the data, with k_{fast} and k_{slow} as 2.4 ± 1.0 and 0.65 ± 0.23 s^{-1} (apo), 4.4 ± 1.6 and 0.21 ± 0.02 s^{-1} (AMPPNP). The corresponding amplitudes of the fast and slow phases were 0.045 ± 0.012 and 0.041 ± 0.010 (apo), 0.023 ± 0.005 and 0.034 ± 0.008 (AMPPNP).

Interestingly, we have indeed found some clues to the effect for other helicases.

In the single turnover DNA unwinding kinetic study of the *dimeric* UvrD helicase using ss/dsDNA substrates of varying tail lengths (Fig. 1 in Ref. 13), the unwinding efficiency increased abruptly with increasing ssDNA tail length flanking the duplex DNA substrate and then reached a peak at 15 nt. A further increase of the tail length to 20 nt, puzzlingly, did not help to augment the efficiency, but rather, made it drop slightly. Then, as the tail length became still longer, the efficiency increased mildly again.

At present we think this phenomenon may be explained by considering the mutual inhibition effect. As the PcrA, UvrD, and Rep helicases are highly homologous, it is reasonable to think that their ssDNA binding site sizes are similar. According to previous crystal structures and titration measurements, their binding site sizes are ~8–9 nt (7, 8, 16, 26). Considering that several base pairs at the ss/dsDNA may be opened by the binding of a helicase (24, 27), we may deduce that the functional dimer occupies ~15 nt of the ssDNA tail, thus has a optimized unwinding efficiency at this tail length. When the tail length is increased to 20 nt, the additional ~5-nt tail provides the opportunity for a third monomer to bind to the ssDNA. It is not difficult to imagine, the two monomers in the leading active dimer may be compressed by binding of the third monomer, resulting in a reduced unwinding efficiency through inhibition of ATP binding to the active dimer. When the tail length further increases above 20 nt, the mutual inhibition effect should still exist with more and more bound monomers, but it is more than counteracted by positive contributions of these trailing monomers to the unwinding efficiency through replacing prematurely dissociated leading helicase. It should be mentioned that the above UvrD experiments were performed with 1 mM ATP. We believe the observed phenomenon could be more obvious at low ATP concentrations.

At this point, one may wonder whether the mutual inhibition effect exists for the two monomers within an active UvrD

dimer. In the lack of structural information, the answer is not known. But if the effect really exists, then it would be an inherent property of the UvrD dimer. But without a doubt, its negative role should be more than compensated for by the positive cooperation of the two monomers during DNA unwinding.

Another superfamily I helicase that seems to reveal the mutual inhibition effect in a similar but less obvious way is PcrA, a homologue to UvrD. In our previous single turnover experiments for PcrA, the DNA unwinding efficiency is somewhat lower than expected for the 20-nt tailed substrate (Fig. 2 in Ref. 16). At that time, we found no reasonable explanation. We only thought that the phenomena observed for UvrD and PcrA very probably resulted from the same unknown reasons.

Interestingly, in our early study of the single turnover unwinding kinetics of RecQ, the unwinding amplitude of the fast phase, which was contributed by RecQ monomers prebound at the ss/dsDNA junctions, also had a strange drop for substrates with long tails (Fig. 5 in Ref. 15). We now understand that this might result from the mutual inhibition effect. In those experiments, the concentration of the ss/dsDNA substrate was 2 nM and that of RecQ was much higher (50 nM), thus the inhibition effect appeared and influenced DNA unwinding. Note, however, that the effect was not very significant there because the ATP concentration used was saturating (1 mM). Therefore, the total unwinding amplitude still increased slightly with the increasing 3′ tail length (or the number of pre-bound RecQ monomers).

In summary, we have observed the mutual inhibition effect of neighboring RecQ monomers in DNA unwinding. The cleft between the two RecA-like domains of one monomer may be forced to be closed prior to ATP binding by a trailing monomer. Then the whole DNA unwinding process may be blocked by prohibition of ATP binding to the leading monomer. The inhibition effect could have resulted from simultaneous binding of several monomers to DNA before unwinding initiation, as clearly demonstrated by the AMPPNP experimental results (Fig. 11). It could also be caused by the forward movement of a trailing monomer in the course of unwinding, as demonstrated by the experiment with 30-bp DNA substrate (Fig. 7), because the ssDNA translocation rate of a helicase is usually higher than its DNA unwinding rate.

In principle, the mutual inhibition effect could apply to all helicases with two RecA-like domains, whether monomeric or dimeric and whether in dsDNA unwinding or ssDNA translation. In dsDNA unwinding, if a helicase has a high processivity and does not easily detach from the DNA substrate, then under single turnover conditions, the effect would only reduce the average unwinding rate by increasing the ATP binding time for the functional helicase at the ss/dsDNA junction, but not the unwinding efficiency (amplitude). On the contrary, if the helicase has a low processivity and detaches from the DNA substrate with a high rate, then under single turnover conditions, the effect would reduce not only the observed average unwinding rate by increasing the ATP binding time, but also the unwinding efficiency via enhancing the dissociation probability. As a result, the actual processivity of the helicase would become even lower due to the inhibition effect. In ssDNA trans-

location, similarly, mutual inhibition could influence both the average translocation rate and processivity.

Currently, more and more structural and kinetic studies support that superfamily I or II helicases may translocate along ssDNA and unwind duplex DNA by utilizing, at least partially, a nucleotide state-modulated relative movement of the two RecA-like domains. We think the mutual inhibition effect represents new direct evidence for such an inchworm mechanism.

REFERENCES

1. Matson, S. W., and Kaiser-Rogers, K. A. (1990) *Annu. Rev. Biochem.* **59,** 289–329
2. Lohman, T. M., and Bjornson, K. P. (1996) *Annu. Rev. Biochem.* **65,** 169–214
3. Patel, S. S., and Picha, K. M. (2000) *Annu. Rev. Biochem.* **69,** 651–697
4. von Hippel, P. H., and Delagoutte, E. (2001) *Cell* **104,** 177–190
5. Singleton, M. R., Dillingham, M. S., and Wigley, D. B. (2007) *Annu. Rev. Biochem.* **76,** 23–50
6. Singleton, M. R., and Wigley, D. B. (2002) *J. Bacteriol.* **184,** 1819–1826
7. Velankar, S. S., Soultanas, P., Dillingham, M. S., Subramanya, H. S., and Wigley, D. B. (1999) *Cell* **97,** 75–84
8. Lee, J. Y., and Yang, W. (2006) *Cell* **127,** 1349–1360
9. Dillingham, M. S., Wigley, D. B., and Webb, M. R. (2000) *Biochemistry* **39,** 205–212
10. Tomko, E. J., Fischer, C. J., Niedziela-Majka, A., and Lohman, T. M. (2007) *Mol. Cell* **26,** 335–347
11. Levin, M. K., Wang, Y. H., and Patel, S. S. (2004) *J. Biol. Chem.* **279,** 26005–26012
12. Ali, J. A., Maluf, N. K., and Lohman, T. M. (1999) *J. Mol. Biol.* **293,** 815–834
13. Maluf, N. K., Fischer, C. J., and Lohman, T. M. (2003) *J. Mol. Biol.* **325,** 913–935
14. Byrd, A. K., and Raney, K. D. (2005) *Biochemistry* **44,** 12990–12997
15. Zhang, X. D., Dou, S. X., Xie, P., Hu, J. S., Wang, P. Y., and Xi, X. G. (2006) *J. Biol. Chem.* **281,** 12655–12663
16. Yang, Y., Dou, S. X., Ren, H., Wang, P. Y., Zhang, X. D., Qian, M., Pan, B. Y., and Xi, X. G. (2008) *Nucleic Acids Res.* **36,** 1976–1989
17. Hickson, I. D. (2003) *Nat. Rev. Cancer* **3,** 169–178
18. Bennett, R. J., and Keck, J. L. (2004) *Crit. Rev. Biochem. Mol. Biol.* **39,** 79–97
19. Xu, H. Q., Deprez, E., Zhang, A. H., Tauc, P., Ladjimi, M. M., Brochon, J. C., Auclair, C., and Xi, X. G. (2003) *J. Biol. Chem.* **278,** 34925–34933
20. Bernstein, D. A., Zittel, M. C., and Keck, J. L. (2003) *EMBO J.* **22,** 4910–4921
21. Ha, T., Rasnik, I., Cheng, W., Babcock, H. P., Gauss, G. H., Lohman, T. M., and Chu, S. (2002) *Nature* **419,** 638–641
22. Rasnik, I., Myong, S., Cheng, W., Lohman, T. M., and Ha, T. (2004) *J. Mol. Biol.* **336,** 395–408
23. Fischer, C. J., Maluf, N. K., and Lohman, T. M. (2004) *J. Mol. Biol.* **344,** 1287–1309
24. Levin, M. K., Gurjar, M., and Patel, S. S. (2005) *Nat. Struct. Mol. Biol.* **12,** 429–435
25. Ha, T. (2001) *Methods* **25,** 78–86
26. Korolev, S., Hsieh, J., Gauss, G. H., Lohman, T. M., and Waksman, G. (1997) *Cell* **90,** 635–647
27. Büttner, K., Nehring, S., and Hopfner, K. P. (2007) *Nat. Struct. Mol. Biol.* **14,** 647–652